Journal of Membrane Science 381 (2011) 192–196

Contents lists available at ScienceDirect

Journal of Membrane Science

journal homepage: www.elsevier.com/locate/memsci

# Computational prediction of durable amorphous metal membranes for $H_2$ purification

Shiqiang Hao, David S. Sholl*

*School of Chemical and Biomolecular Engineering, Georgia Institute of Technology, Atlanta, GA 30332-0100, USA*

ARTICLE INFO

*Article history:*
Received 11 May 2011
Received in revised form 7 July 2011
Accepted 17 July 2011
Available online 22 July 2011

*Keywords:*
Hydrogen
Metal membranes
Amorphous metals
Theory and modeling
Alloys

ABSTRACT

Amorphous metals are interesting candidates as membranes for $H_2$ purification. Identifying materials with high permeability for $H_2$ remains a challenge in this field. We apply recently developed methods that combine first principles density functional theory calculations and statistical mechanics to make predictions of the properties of interstitial H in amorphous metals. Our calculations greatly expand the number of amorphous metals which have been considered as membranes, and predict several materials with promising properties.



## 1. Introduction

Hydrogen has the potential to play an important role in creating large-scale changes to the mix of energy sources used by our global society, particularly in transport applications that currently dependent on liquid hydrocarbons. If hydrogen is to be used in fuel cells for vehicular transport, stringent requirements on the purity of hydrogen must be met. Membrane-based separations using dense metal films provide an excellent strategy for achieving separations from syngas [1]. Even though a large number of binary and multicomponent crystalline alloys have been tested experimentally as metal membranes [2], the search for durable and cost effective alloys that show high permeability for $H_2$ continues to be an active area. A useful benchmark for considering the permeability of new membrane materials is that the permeability of pure Pd when used with pure $H_2$ as the feed gas is $\sim 10^{-8}$ (mol m$^{-1}$ s$^{-1}$ Pa$^{-0.5}$) at 600 K [3].

A number of experimental studies have examined amorphous metal films as membranes for $H_2$ purification [4–6]. Amorphous ZrNi and ZrNiNb films have been shown to have $H_2$ permeabilities comparable to pure Pd [3,4,7–9]. Because the solubility and diffusion of interstitial H in amorphous metals is qualitatively different from crystalline metals [10], amorphous films offer intriguing opportunities as $H_2$ membranes [11,12].

A key challenge in developing new materials as membranes is the need to efficiently screen a variety of candidate materials to find promising examples for more detailed testing. Quantitative theoretical models that make predictions without experimental input can play an important role in this area. Models of this kind based on density functional theory (DFT) calculations for the properties of interstitial H in metals have been used for a number of years to examine crystalline Pd-based alloys [13–16]. We have recently developed and verified a DFT-based computational strategy to predict hydrogen permeation rates through amorphous metals [17,18]. We have shown that our approach gives good agreement with experimental results for amorphous $Zr_{36}Ni_{64}$ and $Zr_{30}(Ni_{0.6}Nb_{0.4})_{70}$ without requiring any experimental input [18]. In this paper, we use these methods to predict $H_2$ permeability through nine amorphous metals with a broad range of compositions. These results greatly expand the number of amorphous metals that have been considered as $H_2$ membranes.

A potential problem with using amorphous films as membranes is that if crystallization occurs, the favorable properties associated with the amorphous structure can be irreversibly lost. To identify materials potentially suitable for $H_2$ purification at 300–500 °C, which are typical for $H_2$ production from hydrocarbons, we surveyed the literature to find amorphous metals with high crystallization temperatures. Information on 269 amorphous metals is given in Fig. 1 and Table S1. To simplify our calculations, we have focused in this work on binary alloys. Two of the binary alloys with high crystallization temperature have already been examined experimentally as membranes [3]: $Ni_{62}Nb_{38}$ (932 K [19]) and $Zr_{35}Ni_{65}$ (863 K [20]). We have performed calculations

* Corresponding author. Tel.: +1 404 894 2822; fax: +1 404 894 2866.
*E-mail address:* david.sholl@chbe.gatech.edu (D.S. Sholl).

0376-7388/$ – see front matter © 2011 Elsevier B.V. All rights reserved.
doi:10.1016/j.memsci.2011.07.026

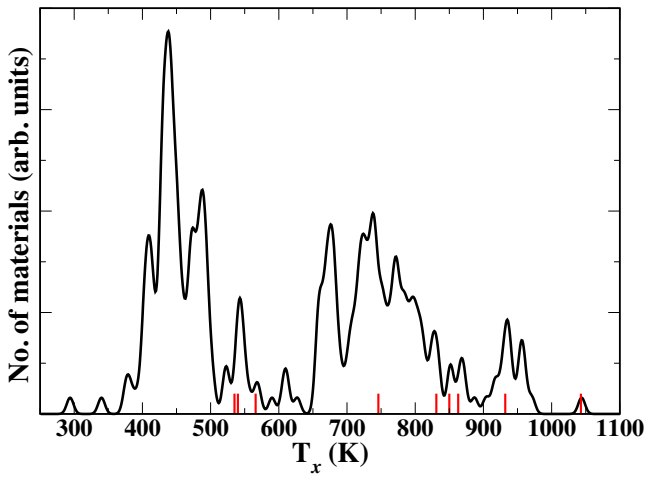


**Fig. 1.** Number of amorphous metals as a function of crystallization temperature. The red sticks label binary phases among which $Ta_{40}Ni_{60}$ (1043 K), $Ni_{62}Nb_{38}$ (932 K), $Zr_{35}Ni_{65}$ (863 K), $Ti_{33}Co_{67}$ (850 K), $Hf_{44}Cu_{56}$ (831 K), and $Zr_{54}Cu_{46}$ (746 K) have $T_x > 700$ K. (For interpretation of the references to color in this figure legend, the reader is referred to the web version of the article.)

for the nine additional binary and ternary materials in Fig. 1 with crystallization temperatures above 700 K: $Ta_{40}Ni_{60}$ (1043 K) [21], $Ta_{25}Ni_{60}Ti_{15}$ (970 K) [21], $Ti_{33}Co_{67}$ (850 K) [22], $Hf_{44}Cu_{56}$ (831 K) [23], $Hf_{25}Cu_{60}Ti_{15}$ (805 K) [24], $Zr_{45}Cu_{45}Al_{10}$ (776 K) [25], $Zr_{30}Cu_{60}Ti_{10}$ (763 K) [26], $Zr_{54}Cu_{46}$ (746 K) [27], and $Nd_{60}Fe_{30}Al_{10}$ (722 K) [19]. Throughout our results, compositions are indicated in at.%.

During $H_2$ purification, hydrogen permeates through a metal film by dissociation of $H_2$, diffusion of atomic H through interstitial sites in the metal, and recombination of atomic H as $H_2$ [1,2]. Throughout our calculations, we consider the common situation where surface dissociation process is not rate limiting and bulk diffusion is rate determining. In experiments with amorphous films, this is often achieved by using a thin layer of Pd as a catalytic layer on the film's surface [12]. When surface processes can be neglected, the net permeability of a film can be predicted if the solubility and diffusivity of H in the bulk material is known [2,13].

## 2. First principles calculations

The details of our DFT calculations for interstitial H in amorphous metals have been described in previous reports [17], so we summarize the main points here. Our calculations were performed with the Vienna *ab initio* Simulation Package (VASP) using plane wave DFT with the PW91 GGA functional [28]. Supercells approximating amorphous samples were prepared using *ab initio* Molecular Dynamics (MD) at 3000 K. These liquid-like samples were then quenched using conjugate gradient relaxation. The liquid state volumes are ~7% greater than the volume of the quenched amorphous samples [29]. Test calculations for $Ta_{40}Ni_{60}$ and $Ta_{25}Ni_{60}Ti_{15}$ indicated that including spin polarization did not affect the calculated energies, so the MD and quenching calculations were performed without spin polarization. Other materials containing magnetic species ($Ti_{33}Co_{67}$, $Zr_{55}Co_{25}Al_{20}$, and $Nd_{60}Fe_{30}Al_{10}$) were calculated with spin polarization for all MD relaxation, binding energy and transition state calculations. Calculations using 32 atom supercells sampled reciprocal space with $3 \times 3 \times 3$ $k$-points. A limited number of materials were also examined with 108 atom supercells, for which only the $\Gamma$-point was used in $k$-space.

Binding sites for interstitial H were optimized in calculations using one H atom per supercell. We used the methods described

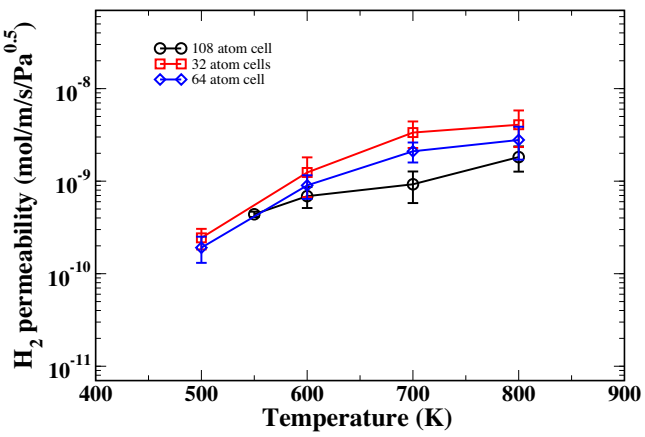


**Fig. 2.** Permeability comparison of $Zr_{55}Co_{25}Al_{20}$ with different sizes of supercell.

elsewhere to efficiently locate all of the interstitial sites and transition states between adjacent interstitial sites for H in the computational volume [30,31]. The procedure normally located 85–95 distinct interstitial sites and 240–290 transition states in each 32 atom supercell. Energies of interstitial sites and transition states were found from DFT calculations that allowed all atomic degrees of freedom in the supercell to relax.

Below, we use DFT-based calculations to predict H solubility and diffusivity in the nine amorphous materials listed above. These calculations are computationally intensive, and the computational effort grows rapidly as the number of atoms in the calculation is increased. In test calculations, we examined $Zr_{55}Co_{25}Al_{20}$ with supercells of 32, 64, and 108 atom cells. As shown in Fig. 2, the permeability predicted with the 32 atom calculations are consistent with (although not identical to) the larger calculations. Motivated by this observation, we used 32 atom supercells to examine the nine candidate materials. We subsequently reexamined the permeability of the four candidates with the highest predicted permeability, $Zr_{54}Cu_{46}$, $Zr_{30}Cu_{60}Ti_{10}$, $Hf_{44}Cu_{56}$, and $Hf_{25}Cu_{60}Ti_{15}$, using 108 atom supercells.

## 3. Results

Our calculations of H solubility in amorphous metals begin by using DFT to compute the binding energy of a single interstitial H in each interstitial site in a sample. Because the solubility of H in these materials can be significant under practical conditions, H–H repulsion plays an important role in determining the overall solubility. We used the Westlake criterion to characterize H–H interactions. This criterion predicts that two interstitial sites separated by less than 0.21 nm cannot be simultaneously occupied by H atoms [32]. We have shown previously that this approach gives results in close agreement with more detailed DFT characterization of H–H interactions in amorphous $Fe_3B$ [30] and ZrNi [18]. With this definition of the binding energy for each interstitial site and description of H–H repulsion, the net solubility of H in our amorphous samples can be calculated as a function of temperature and $H_2$ pressure using Grand Canonical Monte Carlo (GCMC) simulations [30]. These GCMC calculations equate the chemical potential of interstitial H and the gaseous phase, which was treated as an ideal gas. The solubility calculated in this way for $Zr_{54}Cu_{46}$ at two $H_2$ pressures is shown in Fig. 3 in terms of the ratio of H to metal atoms, H/M. There are many conditions where the concentration of H is high. Good agreement can be seen between calculations performed with 32 and 108 atom supercells. A high concentration of interstitial H can induce lattice expansion, and this expansion can affect H binding energies and therefore solubility. We accounted for this effect